

# A Multitechnique Reconfigurable Electrochemical Biosensor for Integration into Mobile Technologies

Alexander Sun, Travis Wambach, A. G. Venkatesh, and Drew A. Hall

Department of Electrical and Computer Engineering  
University of California, San Diego  
La Jolla, CA, USA  
drewhall@ucsd.edu

**Abstract**— This paper describes the design and validation of a reconfigurable, multitechnique electrochemical biosensor intended for direct integration into smartphone and wearable technologies to realize a portable platform for Point-of-Care health monitoring. The reconfigurable potentiostat is able to perform various electrochemical techniques (amperometric, potentiometric, and impedance spectroscopy) and interfaces with several types of interchangeable electrochemical sensors all with a minimal number of components. A prototype of the reconfigurable potentiostat module was developed with discrete components, characterized, and compared against benchtop equipment. To show feasibility as well as flexibility of the platform, the device was used to run pH measurements and a glucose assay with comparable performance.

## I. INTRODUCTION

The leading cause of death and disability in the United States is from chronic illnesses such as heart disease, stroke, cancer, and diabetes, which are the most commonly diagnosed and also the most expensive to treat [1]. One of the main factors for this occurrence is the current heavy reliance on periodic hospital checkups that can increase facilities costs and reduce affordability, especially if frequent assessment or continuous monitoring is required.

Fortunately, recent advances in portable electronics, allow for the design of mobile health (mHealth) technology to continuously monitor patients at the point-of-care (POC). While current and next generation mobile devices already boast an impressive array of integrated health oriented sensors, such as electrocardiogram (ECG) and photoplethysmogram (PPG), there remains a lack of molecular sensors to detect biomarkers. These biomolecular sensors, which can enable applications such as remote or at-home diagnosis of infection, monitoring treatment progression, hydration and fatigue tracking during exercise, and testing food and water safety, offer a much more complete and diagnostically relevant picture of the user's health. While several add-on biosensing modules for mobile phones have been developed that leverage intrinsic hardware (e.g., the camera or audio port), these devices are still external to the phone making them more burdensome to manage and transport than a fully integrated solution, dissuading frequent and daily use [2]–[8]. By integrating biosensors into a smartphone or smartwatch, and leveraging the scalability, cost-effectiveness, and accuracy of electrochemical

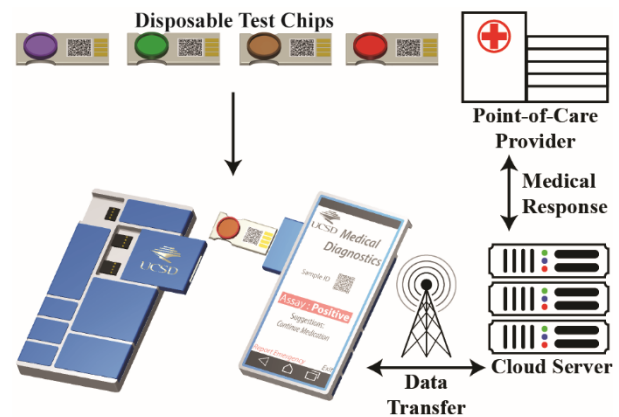


Fig. 1: Complete electrochemical biosensor platform with disposable electrodes, biosensor module, and modular mobile device such as Google ATAP's Project Ara.

biosensing, which led to the success of glucose meter, one can develop much more convenient and seamless mHealth applications that can promote adherence to frequent or continuous testing.

To this end, we describe the design of an electrochemical biosensor module for direct integration into a smartphone through the use of a novel reconfigurable bipotentiostat capable of supporting an extended range of techniques while minimizing the number of required components. The entire system (Fig. 1) has three main components: 1) a disposable test chip, the type of which depends on the application, 2) the reconfigurable potentiostat sensing module, and 3) the mobile platform.

The mobile platform used here is Google ATAP's Project Ara (Spiral 1 prototype) modular smartphone (Fig. 1), which allows the user to swap out different components easily and customize the phone's hardware. This platform is ideal for biosensor integration because of its open and high-speed interface as well as its modularity that enables the smartphone to have biosensing, amongst many other, capabilities.

## II. DESIGN OF THE MODULE

The module (Fig. 2) consists of a potentiostat surrounded by a 4-channel 12-bit DAC and ADC as well as a low-power microcontroller to handle interfacing with the smartphone or wearable. To enable a large set of possible mHealth

This work was supported in part by Google's Advanced Technologies & Projects (ATAP). The views and opinions expressed in this article are those of the authors and do not necessarily reflect that of the funding agency.

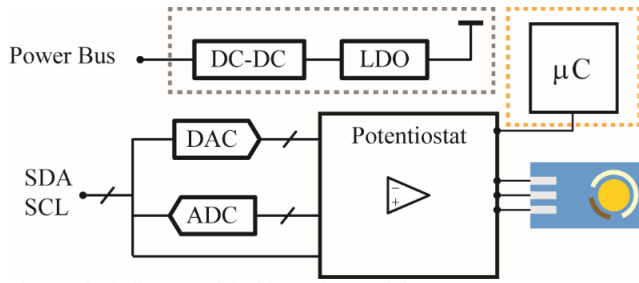


Fig. 2: Block diagram of the biosensing module.

applications, the potentiostat must be able to run multiple types of techniques, which require different sensing modes and additional circuitry. However, space and power are highly constrained resources on a mobile device. Therefore, in order to reduce the area and, more importantly when moving to an integrated circuit implementation, the power, a single reconfigurable design, rather than three different sets of potentiostat circuits, is used that repurposes components from one mode to the next while maintaining performance across different techniques. Hence, the potentiostat (Fig. 2) is designed to be able to change automatically between three different modes: 1) amperometric, 2) potentiometric, and 3) impedance spectroscopy.

This potentiostat has two working electrodes (WE) with each channel having independently configurable gain (10 k $\Omega$ , 100 k $\Omega$ , and 1 M $\Omega$ ) and bandwidth (adding any combination of a 1, 10, and 100 nF capacitor in parallel). This functionality enables two tests to be run in parallel simultaneously on the same sample, allowing one to be a control to compensate for factors such as temperature variation or background signal. Alternatively, the electrodes can be used together for redox cycling with an interdigitated electrode in order to chemically amplify the signal to provide higher sensitivity, particularly when dealing with micro- and nano-scale sensors [9]. Each of these modes and their requirements are explained in the following sections.

#### A. Amperometric Mode

In amperometry, a voltage signal is applied to the sensor between the reference electrode (RE) and the WE, with the counter electrode (CE) supplying the current to set the solution potential. This voltage waveform generates a current signal in the solution that is measured at the WE. These set of techniques are the most widely used and include cyclic voltammetry (CV), chronoamperometry (CA), square wave voltammetry (SWV), and differential pulse voltammetry (DPV). The simplified schematic of this mode is shown in Fig. 3a. Strategically placed multiplexers allow the circuit to be switched at nodes that do not affect performance.

A summary of the specifications are shown in Table I. Since the sensitivity of these measurements depends on how accurately current can be measured, the most important design considerations for this mode are the input-referred noise, which was measured with 100 k $\Omega$  gain and a 1 kHz bandwidth, and the input bias current of the transimpedance amplifier (TIA). Since low leakage multiplexors ( $\sim 5$  pA) for

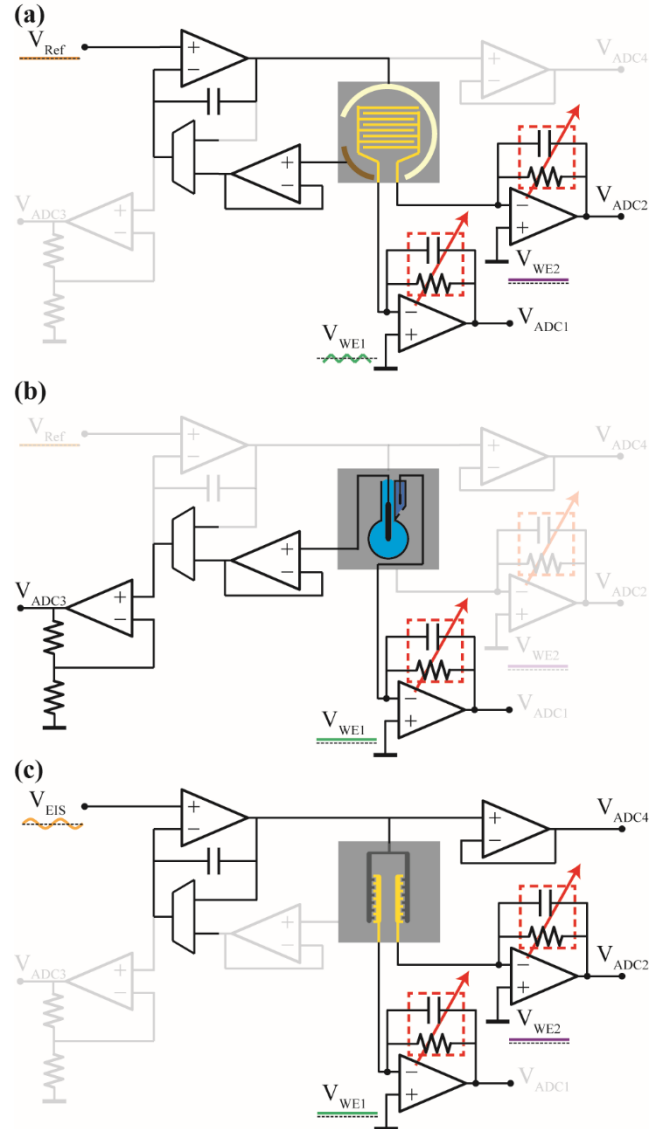


Fig. 3: Schematic of a) Amperometric, b) potentiometric, and c) impedance spectroscopy modes.

selecting the gain and bandwidth are used and the number of mux inputs connected to the inverting node are minimized, the overall input leakage for the TIA is dominated by the input bias current of the op-amp. Hence, we can measure currents in the sub-nA range, sufficient for most applications which tend to be anywhere from a bidirectional 100  $\mu$ A to 1 pA, depending on the type and size of the sensor used. Furthermore, the input bias current of the RE circuitry must be minimized in order to reduce the IR error of the applied voltage, which affects the accuracy of the voltage applied between the electrodes. By using a very low input bias op-amp, this design achieves an RE leakage of 200 fA, which, with a typical solution resistance of 100  $\Omega$ , contributes a negligible 100 nV error.

#### B. Potentiometric Mode

In the potentiometric mode (Fig. 3b), the voltage generated between two electrodes in a solution is measured. Typically,

TABLE I. SPECIFICATIONS FOR EACH MODE

Amperometric	
Sensitivity	< 1 nA
Dynamic Range	60 dB (1 nA – 1 $\mu$ A)
Input-Referred Noise	216 pA <sub>RMS</sub> (0.1 Hz – 1 kHz)
Input Bias Current (RE)	~200 fA
Input Bias Current (WE)	170 pA
Potentiometric	
Leakage Current	~200 fA
Input Impedance	~20 T $\Omega$
Input-Referred Noise	1.06 $\mu$ V <sub>RMS</sub> (0.1-10 Hz)
Dynamic Range	66 dB (1 mV- 2 V)
Impedance Spectroscopy	
Bandwidth	0.1 Hz – 100 kHz
Maximum AC Current	$\pm$ 5 mA

an ion-selective electrode (ISE) is used, often to measure pH or specific ion concentrations. These electrodes have very large resistances, in the 100 M $\Omega$  range, and require circuitry with an input bias current of less than 1 pA (this design is 200 fA) to ensure that measurement error is less than 1%. Without adding a new set of components, the input buffer used for RE in the amperometric mode is switched into the signal path for use as a high impedance input. This is the same path used for the RE in amperometric modes.

### C. Impedance Spectroscopy

In the electrochemical impedance spectroscopy (EIS) mode, a small-signal voltage of varying frequency is applied between the RE and WE in the test solution. The phase and amplitude of the resulting current signal is used to determine the complex impedance of the solution across different frequencies, typically in the range of 0.1 Hz to 100 kHz. Known test impedances can be connected in between the two electrodes in order to characterize the phase shift in the signal path and compensate the channel accordingly. Due to the high frequency nature of the input and output signals, the hardware is required to be able to operate at high frequencies, which contrasts greatly with the low frequency signals of the previous two modes. This requires further bandwidth adjustments for the control circuitry as well as the TIA.

### D. Communication Interface

Timing is a critical issue especially for EIS where an exact phase shift must be determined. Hence, precise polling of the ADCs and DACs was accomplished by adding a microcontroller to mediate between the potentiostat and the mobile platform. In addition to achieving proper timing, the microcontroller also allows one to easily adapt this module to fit any standard serial communication protocol, further increasing its utility.

## III. CHEMICAL VERIFICATION

A 5 $\times$ 5 cm prototype of the device, shown in Fig. 4, was tested to verify the functionality and performance. As of now, this prototype does not fit within the required 2 $\times$ 1 module size of Project Ara (44 $\times$ 22 mm) to be able to easily build and debug the board. With smaller component packages and more routing layers on the PCB, there is no reason that this cannot be further miniaturized to meet the size requirements.

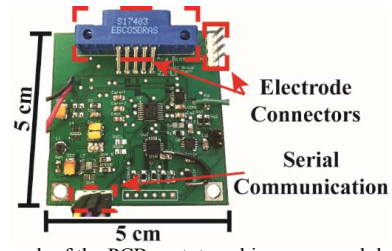


Fig. 4: Photograph of the PCB prototype biosensor module.

### A. Cyclic Voltammetry Comparison

Cyclic voltammetry experiments were conducted with an equal mixture of potassium ferro/ferri-cyanide ( $K_4[Fe(CN)_6]$  /  $(K_3[Fe(CN)_6])$  from Spectrum (P1286, P1296) in a phosphate buffer solution (PBS) of 150 mM potassium phosphate monobasic from Fischer Scientific (P285-500) and potassium phosphate dibasic from EMD Millipore (PX1570-1). 1 mM samples of this solution were applied to gold screen printed electrodes (SPEs) from DropSens. To ensure that we could capture standard voltammograms, cyclic voltammetry measurements, sweeping from -200 mV to 400 mV while varying the scan rate, were made with both the module biosensor and a benchtop potentiostat (CHI 750E) from CH Instruments (Fig. 5a). The analyzed results show the

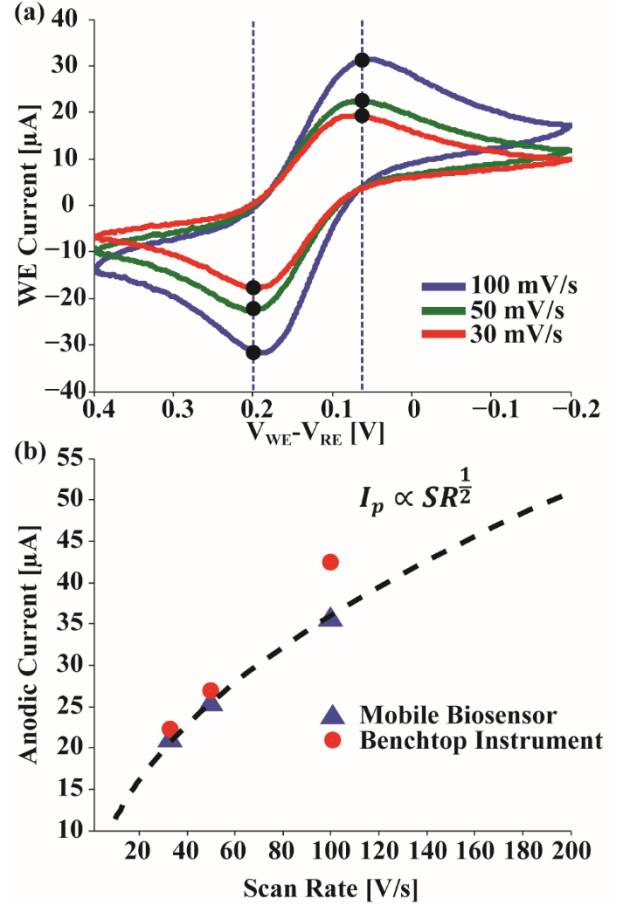


Fig. 5: a) Voltammograms at different scan rates, b) the anodic current peak plotted against scan rate measured by both the module and CHI.

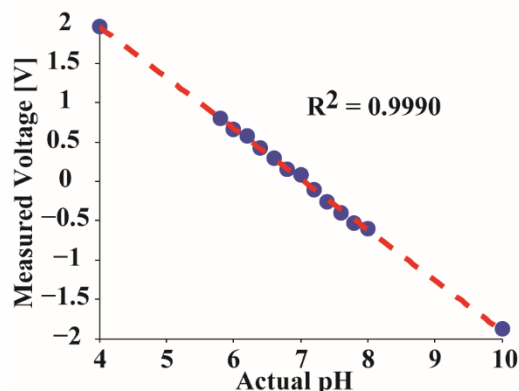


Fig. 6: pH calibration curve with fitted line.

characteristic anodic (200 mV) and cathodic (60 mV) peak voltages match with that of the CHI. Furthermore, the relationship between the scan rate and peak current (Fig. 5b) fits the Randles-Sevcik equation.

### B. pH Measurements

For pH measurements, standard pH buffers from Thermo Scientific (910104, 910107, and 910110) were used as well as prepared phosphate buffers adjusted to specific values ranging from pH 4-10. All measurements were taken with an Oakton pH Probe (EW-35811-74). These buffers were measured with the biosensor module in potentiometric mode and verified

with a table top pH meter (Orion Star A211). The results, as seen in Fig. 6, show a strong linear relationship between the measured voltage and actual pH, as expected.

### C. Glucose Measurements

For Glucose experiments, PBS was spiked with various concentrations of Dextrose from Marcon (4912-12) to create the test solutions. Commercial glucose test strips (True Test Blood Glucose Strips) based on Glucose dehydrogenase-PQQ (GDH) were applied with the various test solutions (27-450 mg/dL) and measured with chronoamperometry (0.5 V step for 10 seconds) with both the CHI and the biosensor module. The results (Fig. 7) show that the measured currents (taken after 10 seconds) for each concentration measured by both instruments follow the same trend. The calibration curve demonstrates that the assay is in the correct region to be able to diagnose or monitor diabetes (positive above 200 mg/dL according to the American Diabetes Association).

## IV. CONCLUSION

We have implemented and demonstrated a reconfigurable, multitechnique biosensor platform designed for integration into Project Ara and possibly other mobile devices for monitoring and diagnosing a user at the POC. We hope to add further sensors while improving cost and form factor, thereby creating specialized, portable, and practical medical devices well positioned to be the first line of defense in the future of healthcare.

## REFERENCES

- [1] B. W. Ward, J. S. Schiller, and R. A. Goodman, "Multiple Chronic Conditions Among US Adults: A 2012 Update," *Prev. Chronic. Dis.*, vol. 11, Apr. 2014.
- [2] A. Nemiroski, D. C. Christodouleas, J. W. Hennek, A. A. Kumar, E. J. Maxwell, M. T. Fernández-Abedul, and G. M. Whitesides, "Universal mobile electrochemical detector designed for use in resource-limited applications," *Proc. Natl. Acad. Sci.*, vol. 111, no. 33, pp. 11984–11989, Aug. 2014.
- [3] P. B. Lillehoj, M.-C. Huang, N. Truong, and C.-M. Ho, "Rapid electrochemical detection on a mobile phone," *Lab. Chip*, vol. 13, no. 15, pp. 2950–2955, Jul. 2013.
- [4] A. Sun, T. Wambach, A. G. Venkatesh, and D. A. Hall, "A low-cost smartphone-based electrochemical biosensor for point-of-care diagnostics," in *2014 IEEE Biomedical Circuits and Systems Conference (BioCAS)*, 2014, pp. 312–315.
- [5] V. Oncescu, D. O'Dell, and D. Erickson, "Smartphone based health accessory for colorimetric detection of biomarkers in sweat and saliva," *Lab. Chip*, vol. 13, no. 16, pp. 3232–3238, Jul. 2013.
- [6] V. Oncescu, M. Mancuso, and D. Erickson, "Cholesterol testing on a smartphone," *Lab. Chip*, vol. 14, no. 4, pp. 759–763, Jan. 2014.
- [7] M. Zangheri, L. Cevenini, L. Anfossi, C. Baggiani, P. Simoni, F. Di Nardo, and A. Roda, "A simple and compact smartphone accessory for quantitative chemiluminescence-based lateral flow immunoassay for salivary cortisol detection," *Biosens. Bioelectron.*, vol. 64, pp. 63–68, Feb. 2015.
- [8] S. K. J. Ludwig, H. Zhu, S. Phillips, A. Shiledar, S. Feng, D. Tseng, L. A. van Ginkel, M. W. F. Nielen, and A. Ozcan, "Cellphone-based detection platform for rbST biomarker analysis in milk extracts using a microsphere fluorescence immunoassay," *Anal. Bioanal. Chem.*, vol. 406, no. 27, pp. 6857–6866, Jun. 2014.
- [9] J. Das, K. Jo, J. W. Lee, and H. Yang, "Electrochemical Immunosensor Using p-Aminophenol Redox Cycling by Hydrazine Combined with a Low Background Current," *Anal. Chem.*, vol. 79, no. 7, pp. 2790–2796, Apr. 2007.

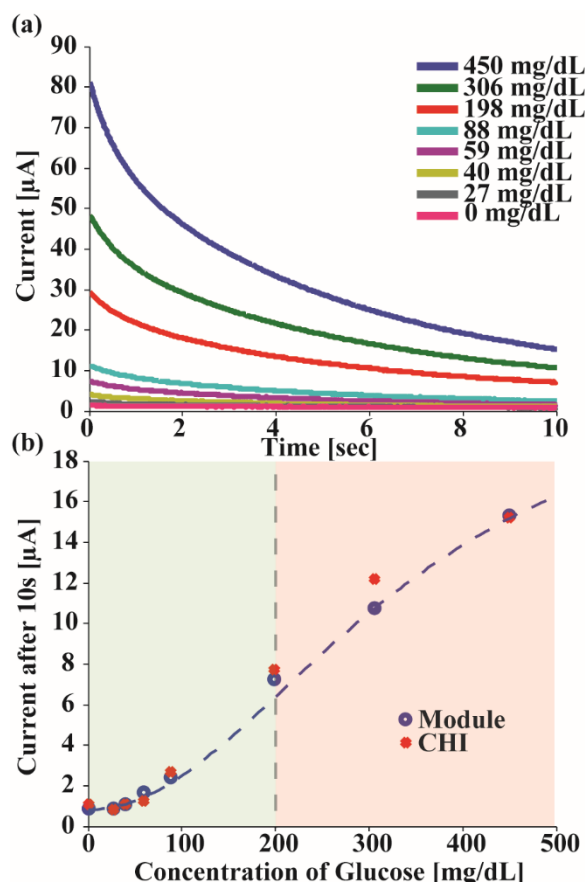


Fig. 7: a) Chronoamperometry curves for glucose measured by the sensing module and b) calibration curves for both the biosensor and CHI with the positive and negative diagnosis ranges annotated.